Secure Transmission in Cell-Free Massive MIMO with RF Impairments and Low-Resolution ADCs/DACs

Xianyu Zhang, Tao Liang, Kang An, Gan Zheng, *Fellow, IEEE,* and Symeon Chatzinotas, *Senior Member, IEEE*

***Abstract*—This paper considers the secure transmission in a cell-free massive MIMO system with imperfect radio frequency (RF) chains and low-resolution analog-to-digital converters (ADCs) and digital-to-analog converters (DACs) at both access points (APs) and legitimate users, where an active eavesdropper attempts to wiretap the confidential data. The Gaussian RF impairment model (GRFIM) and additive quantization noise model (AQNM) are used to evaluate the impacts of the RF impairments and low resolution ADCs/DACs, respectively. The analytical results of the linear minimum mean square error (MMSE) channel estimation show that there is nonzero floor on the estimation error with respect to the RF impairments, ADC/DAC precision and the pilot power of the eavesdropper which is different from the conventional case with perfect transceiver. Then, a tractable closed-form expression for the ergodic secrecy rate is obtained with respect to key system parameters, such as the antenna number per AP, the AP number, user number, quality factors of the ADC/DAC and the RF chain, pilot signal power of the eavesdropper, etc. Moreover, a compensation algorithm between the imperfect RF components and the inexpensive coarse ADCs/DACs is also presented. Finally, numerical results are provided to illustrate the efficiency of the achieved expressions and the devised algorithm, and show the effects of RF impairments and low resolution ADC/DAC on the secrecy performance.**

***Index Terms*—Cell-free massive MIMO, physical layer security, RF impairments, low-resolution ADCs, low-resolution DACs, active eavesdropping.**

I. Introduction

MASSIVE multiple-input multiple-output (MIMO) is an emerging paradigm for the fifth generation (5G) and beyond fifth generation (B5G) wireless networks, which can provide significant spectral and energy efficiency by deploying a large number of antennas at the base station or user equipment [1], [2]. However, deployment of large-scale antennas on a single base station, i.e., co-located massive MIMO, is a major challenge in practical deployment, whose huge antenna array will also lead to high channel correlation [3]. Distributed massive MIMO is a promising alternative which installs several distributed antenna sets onto different geographical locations [4]. As a scalable implementation of the distributed system, cell-free massive MIMO can provide significant advantages in terms of throughput and service coverage through a larger number of geographically distributed access points (APs) [5], [6]. Recently, various contributions in existing literatures, including performance analysis, full-duplex system, relaying communication, power allocation etc, have been presented on cell-free massive MIMO systems [7], [8], [9], [10].

Due to the open nature of the wireless channels, security is a critical issue in wireless communication systems [11]. As a complement of conventional cryptography techniques, physical layer security can be exploited to enhance secure wireless transmission, which has attracted significant research interest in recent years [12]. Because of the abundance of antennas, massive MIMO has the potential in improving physical layer security [13]. Until now, several works have been presented on physical layer security in co-located massive MIMO system, such as multi-cell system, relay massive MIMO system, etc [14], [15], [16], [17], [18]. In addition, secure transmit and security-constrained power allocation in multi-user distributed massive MIMO system have been investigated in [19] and [20]. For cell-free massive MIMO systems, the authors in [21] studied the secure transmission and power control under active pilot spoofing attacks. Besides, the secure communication in multigroup multicasting cell-free massive MIMO systems against active spoofing attack has been investigated in [22]. Secure transmission for simultaneous wireless information and power transfer (SWIPT) cell-free massive MIMO with active eavesdropper has been studied in [23].

Most prior works adopted a common assumption that all APs and users are equipped with perfect radio frequency (RF) chains, analog-to-digital converters (ADCs) and digital-to-analog converters (DACs). However, with the increase of APs in cell-free massive MIMO systems, applying high-quality hardware and high resolution ADCs/DACs bring significant financial costs and energy consumption. From the security perspective, the impacts of hardware impairments on secure co-located massive MIMO systems have been studied in detail in [24] and [25]. In addition, the effect of RF hardware impairments on the physical layer security for cell-free Massive MIMO network has been investigated in [26]. The authors in [27] studied the secrecy performance of the massive MIMO system with low resolution ADCs/DACs in the presence of pilot spoofing attack. The utilization of imperfect transceivers and economical coarse ADCs/DACs is a feasible solution to tackle the bottleneck of cost and energy restriction. For co-

Xianyu Zhang, Tao Liang and Kang An are with the Sixth-third/63rd Research Institute, National University of Defense Technology, Nanjing, 210007 China. (e-mail: zhangxy_sat@126.com, liangtao63@sina.com, ankang89@nudt.edu.cn.)

G. Zheng is with the Wolfson School of Mechanical, Electrical, and Manufacturing Engineering, Loughborough University, Loughborough, U.K. (e-mail: g.zheng@lboro.ac.uk).

S. Chatzinotas is with the Interdisciplinary Centre for Security, Reliability and Trust, University of Luxembourg, Luxembourg (e-mail: symeon.chatzinotas@uni.lu.).

located massive MIMO system, the authors in [28] analyzed the impacts of both RF impairments and ADCs distortions on the channel estimation, capacity, energy efficiency as well as effective compensation algorithms. However, due to general impairment model, there were still residual impairments which should be further incorporated. Utilizing an additive quantization noise model and an extended error vector magnitude model, the uplink achievable rate of massive MIMO system with RF impairments and low resolution ADC has been derived in [29]. Besides, the authors in [30] investigated the uplink achievable rate by considering both the nonideal RF chains and low-resolution ADCs in cell-free massive MIMO system. However, to the best of our knowledge, the secure communication in cell-free massive MIMO system with RF impairments and ADCs/DACs imperfections is still an open issue.

Motivated by the aforementioned observations, this paper considers the secure communication in cell-free massive MIMO system with RF impairments and ADCs/DACs imperfections. The Gaussian RF impairment model (GRFIM) and additive quantization noise model (AQNM) are advocated as suitable models for the RF impairments and ADCs/DACs imperfections, based on which the linear minimum mean square error (MMSE) algorithm is presented for channel estimation [31], [32]. With the adopted RF impairments and ADC imperfections models along with the imperfect channel state information (CSI) assumptions, the closed-form expression of the ergodic secrecy rate has been derived in terms of key design parameters, i.e. pilot and data power, the quality of the RF chains, the precision of the ADCs/DACs, the number of APs and antennas. Besides, the compensation between RF impairments and ADCs/DACs imperfections has been considered and illustrated by simulations. Unlike existing works on secure communication in massive MIMO system which simply considers specific architecture, this paper studies the secure transmission in cell-free massive MIMO sytem with a universal paradigm taking into account the nonideal RF chains, ADCs/DACs distortions and CSI imperfection. The key contributions of this paper are summarized as follows:

- Using the GRFIM and AQNM to model the RF impairments and the ADCs/DACs imperfections, the linear MMSE algorithm is utilized for uplink channel estimation at each AP locally. Based on which, the closed-form statistical properties of the channel estimation and estimation error are provided. Subsequently, each AP can operate the downlink data transmission with the estimated channels.
- The closed-form expressions for the achievable rate of the target user and the Eve are presented, respectively. Then, the closed-form result of the ergodic secrecy rate is derived with respect to key system parameters, such as pilot power, the number of legitimate users and the total antennas, the RF quality factor, the quantization bit of the ADCs/DACs, etc. In general, the closed-form expression can provide generalized and effective insights to evaluate the system parameters on the secrecy performance of the considered system.

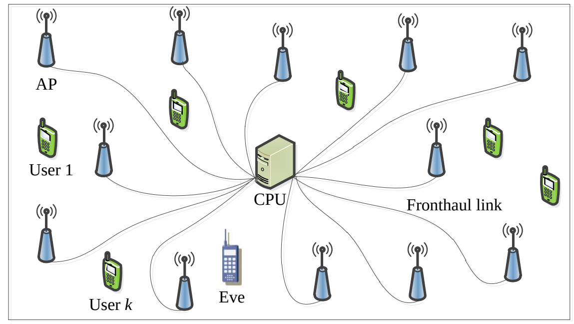

Fig. 1. Illustration of the secure cell-free massive MIMO system.

- To effectively investigate the impacts of the hardware impairments, the compensations between RF impairments and the low resolution ADCs/DACs has been studied in details. That is, different hardware assembling schemes by adjusting the quality factors of the RF chains and ADCs/DACs can achieve the same system performance. Furthermore, an iterative algorithm on performance compensations has been provided and illustrated by simulations.

The outline of the paper is organized as follows. Section II describes the considered secure cell-free massive MIMO system model. Then, the uplink linear MMSE channel estimation is presented in Section III. In Section IV, the downlink data transmission, secrecy performance analysis, and the performance compensations between the RF impairments and coarse ADCs/DACs are discussed in detail. Next, the simulation results are provided in Section V. Finally, Section VI concludes this paper.

Notation: Throughout the paper, boldface lowercase letters and uppercase letters denote vectors and matrices, e.g. $\mathbf{g}$, $\mathbf{G}$. The superscript $(\cdot)^T$, $(\cdot)^*$ and $(\cdot)^H$ express the transpose, conjugate and Hermitian transpose, respectively. $\|\mathbf{g}\|$ ($|g|$) represents the the Euclidean norm (absolute value) of a vector $\mathbf{g}$ (a scalar g). $\mathbb{E}\{\cdot\}$ denote operations of expectation. $\mathrm{diag}(\mathbf{g})$ is a diagonal matrix consisting of diagonal entries of vector $\mathbf{g}$. $[\mathbf{G}]_i$ ($[\mathbf{g}]_i$) represents the ith column vector of the matrix $\mathbf{G}$ (the ith element of the vector $\mathbf{g}$). A circularly symmetric complex Gaussian random vector $\mathbf{x}$ with mean $\mathbf{m}$ and covariance matrix $\mathbf{A}$ can be represented by $\mathbf{x} \sim \mathcal{CN}(\mathbf{m}, \mathbf{A})$. $\mathbf{I}_M$ is $M-$dimensional identity matrix. $\mathbb{C}^{M\times N}$ stands for $M \times N$ dimensional complex space. Besides, i.i.d indicates the abbreviation of independent and identically distributed. RV is the abbreviation of random variable. Finally, $[x]^+ = \max\{0, x\}$.

II. SYSTEM MODEL

As illustrated in Fig. 1, this paper considers a cell-free massive MIMO communication system with M APs (each equipped with N antennas) and K single antenna users in the presence of an active single antenna eavesdropper (Eve) which are all randomly positioned in a certain region. All APs simultaneously serve the K users with the same time-frequency resource and are connected to a central processing unit (CPU) via error-free fronthaul links. By operating in time-division duplex (TDD) mode, the APs can achieve the CSI by uplink

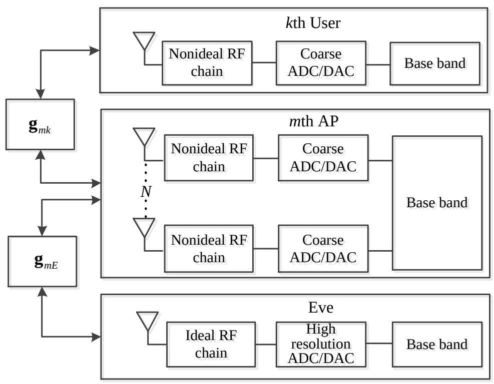

Fig. 2. Architecture of the AP, legitimate user and the Eve.

training by using the channel reciprocity between the uplink and downlink channels. Similar to existing literatures [5], [7], [21], [22], [26], [31], the uncorrelated flat Rayleigh fading channels are advocated in this paper. Specifically, the channel vector between the mth AP and the k_1th ($k_1 = 1, 2, \cdots, K$) user can be denoted by

$$\mathbf{g}_{mk_1} = \sqrt{\beta_{mk_1}}\mathbf{h}_{mk_1}, \tag{1}$$

where β_{mk_1} represents the large-scale fading including path loss and shadowing effects, $\mathbf{h}_{mk_1} \in \mathbb{C}^{N\times 1}$ models the small-scale fading vector with elements being i.i.d. $\mathcal{CN}(0,1)$ RVs. Besides, the channel between the mth AP and the active eavesdropper (Eve) is given by

$$\mathbf{g}_{mE} = \sqrt{\beta_{mE}}\mathbf{h}_{mE}, \tag{2}$$

where β_{mE} is the large-scale fading coefficient, $\mathbf{h}_{mE} \sim \mathcal{CN}(\mathbf{0}, \mathbf{I}_N)$ denotes the corresponding small-scale fading vector.

To further reduce the implementation costs and energy dissipation in cell-free massive MIMO system, this paper considers the economical coarse RF chains and low resolution ADCs/DACs at both the APs and the legitimate users. Furthermore, the eavesdropper can enhance its wiretapping capability by equipping with high quality transceivers and high resolution ADCs/DACs. Hence, this paper makes a worst-case assumption that the Eve is equipped with perfect hardware and ideal ADCs/DACs. The architecture of the APs, legitimate user and the Eve is depicted in Fig. 2.

The secure downlink transmission is considered in this paper. Hence, one coherence interval includes two phases: uplink channel estimation and downlink data transmission.

III. Uplink Channel Estimation

This phase includes the channel estimation through uplink pilots. The large-scale attenuations are assumed constant within each coherence interval and known a priori. Nevertheless, the small-scale fading gains are unknown and needed to be estimated. All K legitimate users simultaneously send pilot sequence to the M APs. Let τ be the uplink pilot sequence duration (in symbols). The pilot signal used by the kth user can be denoted by $\sqrt{\tau}\boldsymbol{\varphi}_k \in \mathbb{C}^{\tau\times 1}$ with $\|\boldsymbol{\varphi}_k\|^2 = 1$. Let P_k be the set of the user indexes which utilize the same pilot signal as the kth user. As a complication in massive MIMO system, the pilot contamination is considered in this paper, that is, different users may utilize the same pilot sequence, i.e. $\tau < K$. Since the pilot sequences are public and repeatedly used, a smart eavesdropper can transmit the same pilot as the target user. Without loss of generality, an assumption can be made that the Eve attempts to wiretap the confidential message to the kth user, i.e. $\boldsymbol{\varphi}_E = \boldsymbol{\varphi}_k$. With an ideal hardware transceiver, the received pilot signal at the mth AP can be represented by

$$\mathbf{Y}_{pm} = \sum_{k_1=1}^{K} \sqrt{\tau p_p}\mathbf{g}_{mk_1}\boldsymbol{\varphi}_{k_1}^H + \sqrt{\tau p_E}\mathbf{g}_{mE}\boldsymbol{\varphi}_k^H + \mathbf{W}_{pm}, \tag{3}$$

where p_p and p_E denote the average transmit pilot power of the legitimate user and the Eve, and $\mathbf{W}_{pm} \in \mathbb{C}^{N\times\tau}$ is the additive white Gaussian noise (AWGN) with elements are i.i.d $\mathcal{CN}(0, \delta^2)$ RVs.

Using the well-established Gaussian RF impairment model (GRFIM) to evaluate the impacts of the coarse RF chains at the users and the APs [32], the received signal can be rewritten as

$$\begin{aligned}\mathbf{Y}_{pm} =& \sqrt{k_A}\sum_{k_1=1}^{K}\mathbf{g}_{mk_1}\left(\sqrt{\tau p_p k_U}\boldsymbol{\varphi}_{k_1}^H + \boldsymbol{\eta}_{k_1 t}^T\right)\\ &+\sqrt{\tau p_E k_A}\mathbf{g}_{mE}\boldsymbol{\varphi}_k^H + \mathbf{D}_{mr} + \mathbf{W}_{pm},\end{aligned} \tag{4}$$

where $k_U \in [0,1]$ and $k_A \in [0,1]$ represent the RF hardware quality coefficients of the legitimate users and the APs, respectively. $\boldsymbol{\eta}_{k_1 t}$ and $\mathbf{D}_{mr}$ model the distortion noise at the transceiver of the k_1th user and the mth AP which are distributed as $\boldsymbol{\eta}_{k_1 t} \sim \mathcal{CN}(0, p_p(1-k_U)\mathbf{I}_\tau)$ and $[\mathbf{D}_{mr}]_i \sim \mathcal{CN}\left(0, p_p(1-k_A)\sum\limits_{k_1=1}^{K}\mathrm{diag}\left(|[\mathbf{g}_{mk_1}]_1|^2, \cdots, |[\mathbf{g}_{mk_1}]_N|^2\right)\right)$, $1 \le i \le \tau$.

For analytical tractability, the popular additive quantization noise model (AQNM) is utilized to quantize the output of the poor-resolution DAC[31]. Furthermore, the received signal through the low-resolution DAC at the mth AP is given by

$$\tilde{\mathbf{Y}}_{pm} = \alpha_A\mathbf{Y}_{pm} + \tilde{\mathbf{W}}_{pm}, \tag{5}$$

where α_A is the quantization factor at the APs which is determined by the quantization bits number of the DAC, b_A. Besides, $\tilde{\mathbf{W}}_{pm}$ is the additive Gaussian quantization noise at the mth AP whose covariance matrix is approximated as [30], [33], [34]

$$\mathbf{R}_{\tilde{\mathbf{W}}_{pm}} \approx \alpha_A(1-\alpha_A)\,\mathrm{diag}\left(\mathbb{E}\left\{\mathbf{Y}_{pm}\mathbf{Y}_{pm}^H\right\}\right). \tag{6}$$

Furthermore, all APs are assumed to be equipped with the same ADCs. The values of α_A are discrete and related to quantization bits b_A. For $b_A \le 5$, the accurate values of α_A can be checked in Table I in [35]. While for $b_A > 5$, α_A can be approximated as

$$\alpha_A = 1 - \frac{\pi\sqrt{3}}{2}2^{-2b_A}. \tag{7}$$

Then, projecting $\tilde{\mathbf{Y}}_{pm}$ onto $\boldsymbol{\varphi}_{k'}$, the post-processing signal can be given by

$$\tilde{\mathbf{y}}_{pm,k'} = \alpha_A\sqrt{k_A}\sum_{k_1=1}^{K}\mathbf{g}_{mk_1}\left(\sqrt{\tau p_p k_U}\boldsymbol{\varphi}_{k_1}^H\boldsymbol{\varphi}_{k'} + \eta_{k_1t,k'}\right) + \alpha_A\sqrt{\tau p_E k_A}\mathbf{g}_{mE}\boldsymbol{\varphi}_k^H\boldsymbol{\varphi}_{k'} + \alpha_A\boldsymbol{\eta}_{mr,k'} + \alpha_A\mathbf{w}_{pm,k'} + \tilde{\mathbf{w}}_{pm,k'}, \tag{8}$$

where $\eta_{k_1t,k'} = \boldsymbol{\eta}_{k_1t}^T\boldsymbol{\varphi}_{k'} \sim \mathcal{CN}\left(0, p_p\left(1-k_U\right)\right)$, $\mathbf{w}_{pm,k'} = \mathbf{W}_{pm}\boldsymbol{\varphi}_{k'}$, $\tilde{\mathbf{w}}_{pm,k'} = \tilde{\mathbf{W}}_{pm}\boldsymbol{\varphi}_{k'}$, the distribution of $\boldsymbol{\eta}_{mr,k'}$ is shown as (9) at the top of the next page.

Theorem 1: Adopting the linear MMSE method at the mth AP, the estimation of the channel vector $\mathbf{g}_{mk'}$ can be given by

$$\hat{\mathbf{g}}_{mk'} = c_{mk'}\tilde{\mathbf{y}}_{pm,k'}, \tag{10}$$

where $c_{mk'}$ can be given by (11) shown at the top of the next page.

In association with these results, the expectation of the norm-square of the channel estimate $\hat{\mathbf{g}}_{mk'}$ and estimation error $\tilde{\mathbf{g}}_{mk'}$ satisfy

$$\mathbb{E}\left\{\|\hat{\mathbf{g}}_{mk'}\|^2\right\} = N\lambda_{mk'}, \tag{12}$$

$$\mathbb{E}\left\{\|\tilde{\mathbf{g}}_{mk'}\|^2\right\} = N\left(\beta_{mk'} - \lambda_{mk'}\right), \tag{13}$$

where $\lambda_{mk'} = \alpha_A\sqrt{k_A k_U \tau p_p}c_{mk'}\beta_{mk'}$.

Proof: Please see Appendix A.

Furthermore, since this paper considers the secure transmission issue, the normalized minimum square error (NMSE) of the channel estimation at the target user can be defined as

$$\text{NMSE} = \frac{\sum\limits_{m=1}^{M}\mathbb{E}\left\{\|\tilde{\mathbf{g}}_{mk}\|^2\right\}}{\sum\limits_{m=1}^{M}\mathbb{E}\left\{\|\mathbf{g}_{mk}\|^2\right\}} = \frac{\sum\limits_{m=1}^{M}\left(\beta_{mk} - \lambda_{mk}\right)}{\sum\limits_{m=1}^{M}\beta_{mk}}. \tag{14}$$

Note that the accuracy of the channel estimation is monotonically increasing in ADC/DAC precision and the RF chain quality.

IV. Secrecy Performance Analysis

In the downlink transmission phase, treating the achieved channel estimate as the true channel parameters, the mth AP performs beamforming for data transmission. Let s_{k_1} be the data intended for the k_1th user with $|s_{k_1}| = 1$, and p_d be the average power constraint at each AP. Similar to some existing works [30], [31], using matched filter locally at each AP, the transmitted signal for all K users at the mth AP can be given by

$$\mathbf{x}_m = \sum_{k_1=1}^{K}\sqrt{p_d k_A\gamma_{mk_1}}\hat{\mathbf{g}}_{mk_1}^* s_{k_1} + \boldsymbol{\eta}_{m,t}, \tag{15}$$

where γ_{mk_1} denotes the power control coefficient corresponding to the power from the mth AP to k_1th user. Considering the power constraint on the mth AP, the power control coefficients should satisfy

$$\sum_{k_1=1}^{K}\gamma_{mk_1}\lambda_{mk_1} \le \frac{1}{N}, m = 1,\cdots,M. \tag{16}$$

Besides, k_A is the RF quality factor of the APs, $\boldsymbol{\eta}_{m,t}$ denotes the RF distortion noise at the mth AP with distribution as (17) at the top of the next page.

As such, considering the RF impairments, the received signal at the kth user and the Eve can be given by

$$r_k = \sqrt{k_U}\sum_{m=1}^{M}\mathbf{g}_{mk}^T\left(\sum_{k_1=1}^{K}\sqrt{k_A\gamma_{mk_1}p_d}\hat{\mathbf{g}}_{mk_1}^* s_{k_1} + \boldsymbol{\eta}_{m,t}\right) + \eta_{k,r} + w_k, \tag{18}$$

$$r_E = \sum_{m=1}^{M}\mathbf{g}_{mE}^T\left(\sum_{k_1=1}^{K}\sqrt{k_A\gamma_{mk_1}p_d}\hat{\mathbf{g}}_{mk_1}^* s_{k_1} + \boldsymbol{\eta}_{m,t}\right) + w_E, \tag{19}$$

where the term $\eta_{k,r}$ models the RF distortion noises at the kth user whose statistical properties can be given by

$$\eta_{k,r} \sim \mathcal{CN}\left(0, \left(1-k_U\right)\sum_{m=1}^{M}\sum_{k_1=1}^{K}\gamma_{mk_1}p_d\left|\mathbf{g}_{mk}^T\hat{\mathbf{g}}_{mk_1}^*\right|^2\right). \tag{20}$$

Besides, $w_k \sim \mathcal{CN}\left(0,\delta^2\right)$ and $w_E \sim \mathcal{CN}\left(0,\delta^2\right)$ are the AWGN at the kth user and the Eve, respectively.

Furthermore, the output signal of the low resolution ADCs at the kth user can be given by

$$\tilde{r}_k = \alpha_U\sqrt{k_U}\sum_{m=1}^{M}\mathbf{g}_{mk}^T\left(\sum_{k_1=1}^{K}\sqrt{k_A\gamma_{mk_1}p_d}\hat{\mathbf{g}}_{mk_1}^* s_{k_1} + \boldsymbol{\eta}_{m,t}\right) + \alpha_U\eta_{k,r} + \alpha_U w_k + \tilde{w}_k, \tag{21}$$

where α_U represents the ADC quantization distortion factor of the legitimate users, $\tilde{w}_k$ is the additive Gaussian quantization noise with covariance as

$$R_{\tilde{w}_k} = \mathbb{E}\left\{|\tilde{w}_k|^2\right\} = \alpha_U\left(1-\alpha_U\right)\mathbb{E}\left\{|r_k|^2\right\}. \tag{22}$$

Then, we focus on the achievable closed-form capacity expressions of the target user and Eve. Furthermore, the ergodic rate is appropriate for the system performance evaluation and has been exploited in many existing works. This paper also utilizes the achievable ergodic secrecy rate for performance measure. Due to the RF chain distortion and coarse ADCs/DACs, the channel estimation and terms at the right of (21) are non-Gaussian distributed which causes the standard capacity analysis impossible. Fortunately, the use-and-then-forget methodology can be used for capacity analysis. In particular, the received signal can be rewritten as

$$\tilde{r}_k = DS_k\cdot s_k + BU_k\cdot s_k + \sum_{k'\neq k}^{K}UI_{kk'}\cdot s_{k'} + HI_t^{AP} + HI_r^{UE} + AN_k + FN_k, \tag{23}$$

where

$$DS_k = \mathbb{E}\left\{\alpha_U\sqrt{\rho_d k_U k_A}\sum_{m=1}^{M}\gamma_{mk}^{1/2}\hat{\mathbf{g}}_{mk}^H\mathbf{g}_{mk}\right\}, \tag{24}$$

$$BU_k = \alpha_U\sqrt{\rho_d k_U k_A}\sum_{m=1}^{M}\gamma_{mk}^{1/2}\hat{\mathbf{g}}_{mk}^H\mathbf{g}_{mk} - DS_k, \tag{25}$$

$$\boldsymbol{\eta}_{mr,k'} \sim \mathcal{CN}\left(0,(1-k_A)\left(p_p\sum_{k_1=1}^{K}\mathrm{diag}\left(\left|[\mathbf{g}_{mk_1}]_1^2,\cdots,[\mathbf{g}_{mk_1}]_N^2\right|\right)+p_E\mathrm{diag}\left(\left|[\mathbf{g}_{mE}]_1^2,\cdots,[\mathbf{g}_{mE}]_N^2\right|\right)\right)\mathbf{I}_\tau\right) \tag{9}$$

$$c_{mk'} = \frac{\sqrt{\tau\rho_p k_A k_U}\beta_{mk'}}{\rho_p\sum\limits_{k_1=1}^{K}\beta_{mk_1}\left(\tau k_A k_U\left|\boldsymbol{\varphi}_{k'}^H\boldsymbol{\varphi}_{k_1}\right|^2+1-k_A k_U\right)+\left(\tau k_A\left|\boldsymbol{\varphi}_{k'}^H\boldsymbol{\varphi}_{k}\right|^2+1-k_A\right)\rho_E\beta_{mE}+\delta^2} \tag{11}$$

$$\eta_{m,t} \sim \mathcal{CN}\left(\mathbf{0},(1-k_A)\,p_d\sum_{k_1=1}^{K}\gamma_{mk_1}\mathrm{diag}\left(\left|[\hat{\mathbf{g}}_{mk_1}]_1^2,\cdots,[\hat{\mathbf{g}}_{mk_1}]_N^2\right|\right)\right) \tag{17}$$

$$UI_{kk'} = \alpha_U\sqrt{\rho_d k_U k_A}\sum_{m=1}^{M}\gamma_{mk'}^{1/2}\hat{\mathbf{g}}_{mk'}^H\mathbf{g}_{mk}, \tag{26}$$

$$HI_t^{AP} = \alpha_U\sqrt{k_U}\sum_{m=1}^{M}\mathbf{g}_{mk}^T\eta_{m,t}, \tag{27}$$

$$HI_r^{UE} = \alpha_U\eta_{kr}, \tag{28}$$

$$AN_k = \alpha_U w_k, \tag{29}$$

$$FN_k = \tilde{w}_k. \tag{30}$$

Also, it can be proved that the terms in (23) are pair-wisely uncorrelated. Then, we can derive the results as follows.

Theorem 2: Using the GRFIM and AQNM to model the imperfect RF chains and low-resolution ADCs/DACs, the expectations of the norm-square of the sum inner product and the norm-square of the Hadamard product of $\sqrt{\gamma_{mk'}}\hat{\mathbf{g}}_{mk'}$ and $\mathbf{g}_{mk}$ can be derived as

$$\begin{aligned}\Omega_{kk'} &= \mathbb{E}\left\{\left|\sum_{m=1}^{M}\sqrt{\gamma_{mk'}}\hat{\mathbf{g}}_{mk'}^H\mathbf{g}_{mk}\right|^2\right\} = \\ & N^2\left(\frac{1-k_U}{\tau k_U}+\left|\boldsymbol{\varphi}_{k'}^H\boldsymbol{\varphi}_k\right|^2\right)\left(\sum_{m=1}^{M}\sqrt{\gamma_{mk'}}\lambda_{mk'}\frac{\beta_{mk}}{\beta_{mk'}}\right)^2 \\ & + N\alpha_A^2\rho_p(1-k_A)\sum_{m=1}^{M}\gamma_{mk'}c_{mk'}^2\beta_{mk}^2 \\ & + N\sum_{m=1}^{M}\gamma_{mk'}\lambda_{mk'}\beta_{mk},\end{aligned} \tag{31}$$

$$\begin{aligned}\Psi_{kk'} &= \mathbb{E}\left\{\left|\sum_{m=1}^{M}\sqrt{\gamma_{mk'}}\hat{\mathbf{g}}_{mk'}^H\circ\mathbf{g}_{mk}\right|^2\right\} = \\ & N\left(\frac{1-k_U}{\tau k_U}+\left|\boldsymbol{\varphi}_{k'}^H\boldsymbol{\varphi}_k\right|^2\right)\left(\sum_{m=1}^{M}\sqrt{\gamma_{mk'}}\lambda_{mk'}\frac{\beta_{mk}}{\beta_{mk'}}\right)^2 \\ & + N\alpha_A^2\rho_p(1-k_A)\sum_{m=1}^{M}\gamma_{mk'}c_{mk'}^2\beta_{mk}^2 \\ & + N\sum_{m=1}^{M}\gamma_{mk'}\lambda_{mk'}\beta_{mk}.\end{aligned} \tag{32}$$

As such, the exact closed-form expression for the achievable ergodic rate of the kth user can be deduced as (33) shown at the top of the next page, where the terms are formulated as

$$DS_k = N\alpha_U\sqrt{\rho_d k_U k_A}\sum_{m=1}^{M}\gamma_{mk}^{1/2}\lambda_{mk}, \tag{34}$$

$$\mathbb{E}\left\{|BU_k|^2\right\} = \alpha_U^2\rho_d k_U k_A\Omega_{kk} - |DS_k|^2, \tag{35}$$

$$\mathbb{E}\left\{|UI_{kk'}|^2\right\} = \alpha_U^2\rho_d k_U k_A\Omega_{kk'}, \tag{36}$$

$$\mathbb{E}\left\{\left|HI_t^{AP}\right|^2\right\} = \alpha_U^2\rho_d k_U(1-k_A)\sum_{k'=1}^{K}\Psi_{kk'}, \tag{37}$$

$$\begin{aligned}\mathbb{E}\left\{\left|HI_r^{UE}\right|^2\right\} &= \alpha_U^2\rho_d(1-k_U)\cdot \\ &\left(k_A\sum_{k'=1}^{K}\Omega_{kk'}+(1-k_A)\sum_{k'=1}^{K}\Psi_{kk'}\right),\end{aligned} \tag{38}$$

$$\mathbb{E}\left\{|AN_k|^2\right\} = \alpha_U^2\delta^2, \tag{39}$$

$$\begin{aligned}\mathbb{E}\left\{|FN_k|^2\right\} &= \alpha_U(1-\alpha_U)\cdot \\ &\left(k_A\rho_d\sum_{m=1}^{M}\Omega_{kk'}+(1-k_A)\rho_d\sum_{m=1}^{M}\Psi_{kk'}+\delta^2\right).\end{aligned} \tag{40}$$

Proof: Please see Appendix B.

Furthermore, for facilitating the analysis of the secrecy performance, an assumption can be presented as follows: the Eve has perfect knowledge of its wiretapping channel, which is the worst case of security. In fact, the upper-bound for the ergodic capacity of the Eve can be obtained under this assumption which also has been widely used in [15], [21], [28]. Then, the signal received at the Eve can be rewritten as

$$r_E = DS_E\cdot s_k+\sum_{k'\neq k}^{K}UI_{E,kk'}\cdot s_{k'}+HI_{E,t}^{AP}+w_E, \tag{41}$$

where

$$DS_E = \sqrt{p_d k_A}\sum_{m=1}^{M}\gamma_{mk}^{1/2}\hat{\mathbf{g}}_{mk}^H\mathbf{g}_{mE}, \tag{42}$$

$$R_k = \log_2\left(1+\frac{|DS_k|^2}{\mathbb{E}\left\{|BU_k|^2+\sum\limits_{k'\neq k}^{K}|UI_{kk'}|^2+\left|HI_t^{AP}\right|^2+\left|HI_r^{UE}\right|^2+|AN_k|^2+|FN_k|^2\right\}}\right) \quad (33)$$

$$UI_{E,kk'} = \sqrt{p_d k_A}\sum_{m=1}^{M}\gamma_{mk'}^{1/2}\hat{\mathbf{g}}_{mk'}^H\mathbf{g}_{mE}, \quad (43)$$

$$HI_{E,t}^{AP} = \sum_{m=1}^{M}\eta_{mt}^H\mathbf{g}_{mE}. \quad (44)$$

The first term in (41) is the desired signal, and the other terms are treated as aggregated noise. Also, it is proved that the terms $UI_{E,kk'}$, $HI_{E,t}^{AP}$ and w_E are pair-wisely uncorrelated. Thus, we can consider of the ergodic information capacity of the Eve as follows.

Theorem 3: Considering the case that both the APs and the legitimate users are equipped with low resolution ADCs/DACs and imperfect RF chains while the active Eve is with perfect hardware, the expectation of the norm-square of the sum inner product and the Hadamard product of $\sqrt{\gamma_{mk'}}\hat{\mathbf{g}}_{mk'}$ and $\mathbf{g}_{mE}$ are given by

$$\begin{aligned}\Omega_{Ek'} &= \mathbb{E}\left\{\left|\sum_{m=1}^{M}\sqrt{\gamma_{mk'}}\hat{\mathbf{g}}_{mk'}^H\mathbf{g}_{mE}\right|^2\right\}\\ &= N^2\alpha_A^2 k_A\tau\rho_E\left|\boldsymbol{\varphi}_{k'}^H\boldsymbol{\varphi}_k\right|^2\left(\sum_{m=1}^{M}\sqrt{\gamma_{mk'}}c_{mk'}\beta_{mE}\right)^2\\ &+ N\alpha_A^2\rho_E\left(1-k_A\right)\left|\boldsymbol{\varphi}_{k'}^H\boldsymbol{\varphi}_k\right|^2\sum_{m=1}^{M}\gamma_{mk'}c_{mk'}^2\beta_{mE}^2\\ &+ N\sum_{m=1}^{M}\gamma_{mk'}\lambda_{mk'}\beta_{mE},\end{aligned} \quad (45)$$

$$\begin{aligned}\Psi_{Ek'} &= \mathbb{E}\left\{\left|\sum_{m=1}^{M}\sqrt{\gamma_{mk'}}\hat{\mathbf{g}}_{mk'}^H\circ\mathbf{g}_{mE}\right|^2\right\}\\ &= N\alpha_A^2 k_A\tau\rho_E\left|\boldsymbol{\varphi}_{k'}^H\boldsymbol{\varphi}_k\right|^2\left(\sum_{m=1}^{M}\sqrt{\gamma_{mk'}}c_{mk'}\beta_{mE}\right)^2\\ &+ N\alpha_A^2\rho_E\left(1-k_A\right)\left|\boldsymbol{\varphi}_{k'}^H\boldsymbol{\varphi}_k\right|^2\sum_{m=1}^{M}\gamma_{mk'}c_{mk'}^2\beta_{mE}^2\\ &+ N\sum_{m=1}^{M}\gamma_{mk'}\lambda_{mk'}\beta_{mE}.\end{aligned} \quad (46)$$

Then, the upper-bound for the ergodic rate of the Eve can be formulated as

$$R_E = \log_2\left(1+\frac{\mathbb{E}\left\{|DS_E|^2\right\}}{\mathbb{E}\left\{\sum\limits_{k'\neq k}^{K}|UI_{E,kk'}|^2+\left|HI_{E,t}^{AP}\right|^2+|w_E|^2\right\}}\right) \quad (47)$$

where

$$\begin{aligned}\mathbb{E}\left\{|DS_E|^2\right\} &= \mathbb{E}\left\{\left|\sqrt{\rho_d k_A}\sum_{m=1}^{M}\gamma_{mk}^{1/2}\hat{\mathbf{g}}_{mk}^H\mathbf{g}_{mE}\right|^2\right\}\\ &= \rho_d k_A\Omega_{Ek},\end{aligned} \quad (48)$$

$$\begin{aligned}\mathbb{E}\left\{|UI_{E,kk'}|^2\right\} &= \mathbb{E}\left\{\left|\sqrt{\rho_d k_A}\sum_{m=1}^{M}\gamma_{mk'}^{1/2}\hat{\mathbf{g}}_{mk'}^H\mathbf{g}_{mE}\right|^2\right\}\\ &= \rho_d k_A\Omega_{Ek'},\end{aligned} \quad (49)$$

$$\mathbb{E}\left\{\left|HI_{E,t}^{AP}\right|^2\right\} = \rho_d k_U\left(1-k_A\right)\sum_{k'=1}^{K}\Psi_{Ek'}, \quad (50)$$

$$\mathbb{E}\left\{|w_E|^2\right\} = \delta^2. \quad (51)$$

Proof: Please refer to Appendix C.

According to some existing papers [15], [19], [21], the ergodic secrecy rate can be used for secure performance analysis which is appropriate for the delay afford systems over many coherence intervals or many channel realizations. In the end, the ergodic secrecy rate can be defined as follows:

$$R_{\text{sec},k} = \left[R_k - R_E\right]^+, \quad (52)$$

where the closed-form expressions of R_k and R_E have been presented in (33) and (47).

The closed-form expression (52) of the achievable ergodic secrecy rate shows the impacts of the RF impairments and ADC/DAC imperfections. It can be proved that the achievable ergodic secrecy rate is monotonically increasing in quantization distortion factor $\alpha_A(\alpha_U)$ and the RF quality factors $k_A(k_U)$ by computing the derivative of the secrecy rate $R_{\text{sec},k}$. To gain more insight, the compensations between the RF impairments and the resolution of ADCs/DACs can be considered based on the achievable ergodic secrecy rate expression as (52). The compensations imply that the performance loss with low quality RF chains can be compensated by equipping high resolution ADCs/DACs, and vice versa. Unfortunately, due to the complexity of the expressions on channel estimation and the ergodic secrecy rate, it is implicit and challenging to quantify the compensation case and obtain some exact closed-form solutions. In order to obtain useful insights, some special cases can be considered to investigate the compensations. To make the problem analysable, some assumptions can be made as follows: the APs and the legitimate user has the same quality of RF chains and ADCs/DACs, i.e. $\alpha_A = \alpha_U = \alpha$, $k_A = k_U = k$. In this case, the compensation issue can be solved by one-dimensional search method. To achieve some accurate compensation schemes, one iterative search algorithm can be designed as Algorithm 1.

Algorithm 1 Performance compensation algorithm between the RF impairments and the resolution of ADCs/DACs

(1) Initialization: set the initial value (α_0, k_0), the target value α_t and the initial search domain $F \in [f_{\min}, f_{\max}]$, computing the corresponding secrecy rate $R_{\text{sec}}^{(0)}$, bits number as b_0 and b_t, if $b_t > b_0$, set $f_{\min} = f_{\min}^0$=0 and $f_{\max} = f_{\max}^0 = k_0$ elseif $b_t < b_0$, set that $f_{\min} = k_0$ and $f_{\max} = 1$.

(2) Dividing the search region F into Q segments with set as $\left\{f_{\min}, \cdots, f_{\min} + \frac{i}{Q}\left(f_{\max} - f_{\min}\right), \cdots, f_{\max}\right\}$, $0 \le i \le Q$. With the fixed ADC/DAC imperfection factor α_t, computing the corresponding secrecy rate $R_{\text{sec},i}$;
(3) If $R_{\text{sec},i} \le R_{\text{sec}}^{(0)}$ and $R_{\text{sec},i+1} \ge R_{\text{sec}}^{(0)}$, updating the search domain as $f_{\min} = f_{\min}^1 = f_{\min}^0 + \frac{i}{Q}\left(f_{\max}^0 - f_{\min}^0\right)$ and $f_{\max} = f_{\max}^1 = f_{\min}^0 + \frac{i+1}{Q}\left(f_{\max}^0 - f_{\min}^0\right)$, the performance loss caused by low resolution ADCs/DACs cannot be compensated by improving the quality of the RF chains.
(4) Repeat step 2 and step 3 until $\left|R_{\text{sec},i} - R_{\text{sec}}^{(0)}\right| \Big/ \left|R_{\text{sec}}^{(0)}\right| \le \varepsilon$; Then, set that $k_t = f_{\min} + \frac{i}{Q}\left(f_{\max} - f_{\min}\right)$;
(5) Return values (α_t, k_t) as the compensation solution of (α_0, k_0).

V. Simulation Results

In this section, representative simulation results are provided to evaluate the secrecy performance of the considered system. M APs, K legitimate users and the Eve are randomly uniformly distributed in a hexagonal cell region with a radius of 1000m. To investigate the pilot contamination issue, all sequences are non-orthogonal. For facilitating the analysis and design, different pilot sequences are designed orthogonally in the simulations while each pilot signal can be used by K/τ users. In addition, key system parameters in the simulations are set as follows: $M = 200$, $K = 10$, $N = 2$, $\tau = 5$, $p_p = 100\text{mW}$, $p_E = 50\text{mW}$, $p_d = 100\text{mW}$. The large-scale fading coefficient is composed of the path loss and the shadow fading which is modeled as

$$\beta = PL \cdot 10^{\frac{\delta_{sh} z}{10}}, \tag{53}$$

where PL denotes the path loss, $10^{\frac{\delta_{sh} z}{10}}$ represents the shadow fading with standard deviation $\delta_{sh} = 8\text{dB}$ and random variable $z \sim \mathcal{N}(0, 1)$. According to some existing works [5], [7], [21], [22], [26], [31], the three-slope model is used to model the path loss, where the path loss model in dB is represented as

$$PL = \begin{cases} -L - 35\log_{10} d, & \text{if} \quad d > d_1 \\ -L - 15\log_{10} d_1 - 20\log_{10} d, & \text{if} \quad d_0 < d \le d_1 \\ -L - 15\log_{10} d_1 - 20\log_{10} d_0, & \text{if} \quad d \le d_0 \end{cases} \tag{54}$$

where $L = 140.7\text{dB}$, $d_0 = 10\text{m}$, $d_1 = 50\text{m}$.

In accordance with the relevant literature, the noise power at the APs and all users in watt can be given by

$$\delta^2 = B \times k_B \times T_0 \times \text{noise figure}, \tag{55}$$

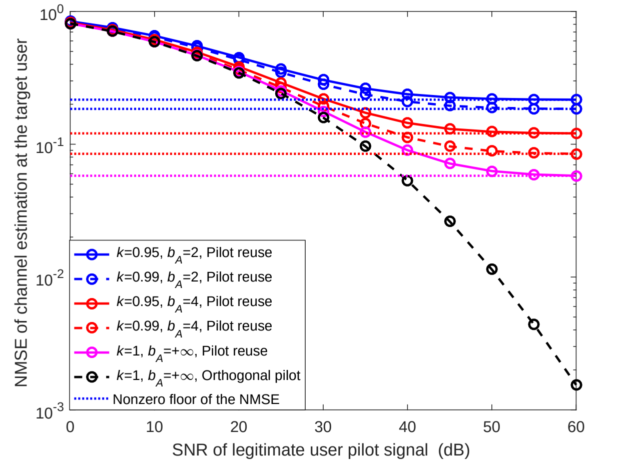

Fig. 3. The NMSE of the channel estimation at the target user versus SNR of the legitimate user pilot signal.

where $k_B = 1.381 \times 10^{-23}\,(\text{J/Kelvin})$, $T_0 = 290\,(\text{Kelvin})$, $B = 20\text{MHz}$, noise figure $= 9\text{dB}$.

Fig. 3 depicts the NMSE of the channel estimation versus the signal-to-noise ratio (SNR) of the legitimate user pilot signal with respect of the RF hardware quality coefficients (k_A and k_U), ADCs/DACs quantization factor α_A at the AP and the pilot attacking power p_E. To facilitate comparison and analysis, we firstly consider the situation that $k_U = k_A$ and $\alpha_U = \alpha_A$. It is noted that the NMSE degrades with the decrease of the transceivers quality, which implies that low resolution ADCs/DACs and RF impairments deteriorate the accuracy of the linear MMSE channel estimation. Since the Eve sends the same pilot signals as the target user, it will degrade the pilot signal reception and increase the channel estimation uncertainty at the APs. Besides, the pilot reuse results in pilot contamination which will lead to a nonzero floor at the channel estimation error. Hence, it can be seen that there are nonzero estimation error floors in the high SNR regime (horizontal dashed lines in Fig. 3) caused by the RF distortions, low resolution ADCs/DACs and the pilot contamination. However, implementing perfect transceivers at the users and APs as well as the orthogonal pilots lead to an error-free channel estimation at high SNR.

Then, we present simulation results to verify the accuracy of the derived secrecy performance merits. Fig. 4 shows the Monte Carlo simulated and analytical results of the R_k and R_E versus M, where the simulated results are obtained by averaging over 5000 independent channel realizations. As expected, more APs yield improved coverage probability, which can be proved by the fact that the achievable ergodic rate of the target user and the ergodic capacity of the Eve are both monotonically increasing with the increase of M. Different from the passive eavesdropper which cannot get distinct benefits by increasing the total antennas [19], the achievable capacity of the active Eve takes advantage of equipping more antennas. It is gratifying to observe that the analytical results are tight with the simulated numerical values in high accuracy. Then, Fig. 5 shows the achievable secrecy rate versus M with different quality of ADC/DAC and RF

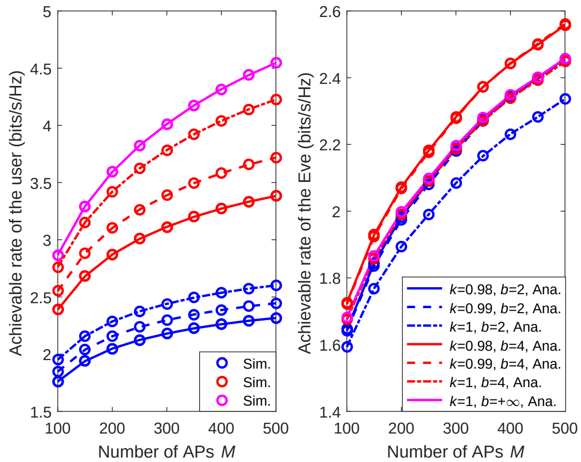

Fig. 4. Analytical (Ana.) and simulated (Sim.) ergodic rates of the target user and the Eve versus the number of the APs M.

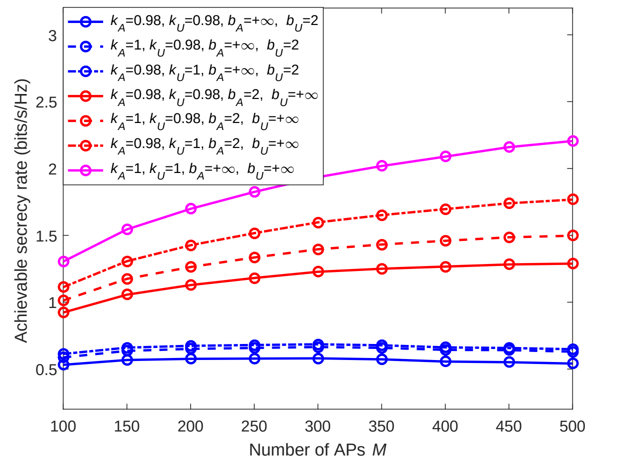

Fig. 6. The achievable ergodic secrecy rates with different hardware equipping schemes.

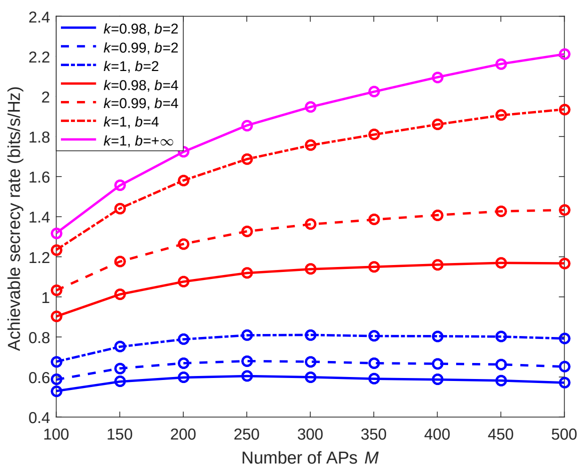

Fig. 5. The achievable ergodic secrecy rates versus the number of the APs M.

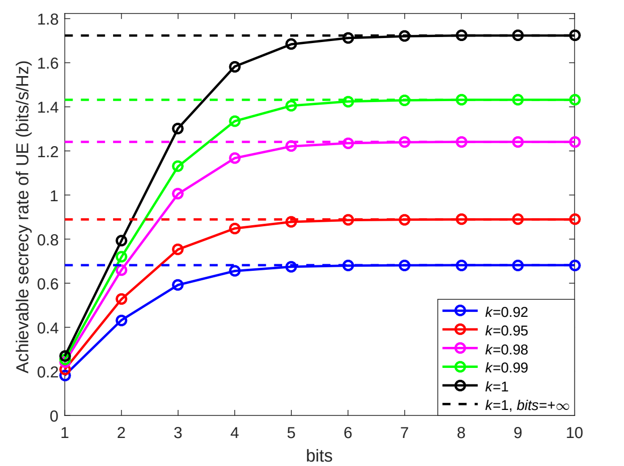

Fig. 7. The achievable ergodic secrecy rates versus the quantization bits of low resolution ADCs.

chains. It is clear that the ergodic secrecy rate reduces as the quantization distortion factors of the ADCs/DACs and the RF quality factors decrease. Besides, we note that the low quality ADCs/DACs and the RF impairments provoke a significant deterioration to the ergodic secrecy rate.

To clarify the effects of RF impairments and ADC/DAC quality, the impacts of hardware quality on users and APs, are shown in Fig. 6 with different hardware equipping schemes (with different k_U, k_A, α_U and α_A). It can be seen that the ergodic secrecy rate decreases with deploying low quality ADC/DAC and RF chains. Nevertheless, it is noted that the quality of the RF chain and ADCs at the legitimate user has a more serious impact on the ergodic secrecy rate since the ergodic secrecy rates with low quality hardware at the users are inferior to the case with the same quality factor at the APs. This observation means that equipping more APs can effectively compensate the performance loss caused by the low quality of APs while it cannot mitigate the detrimental effect of imperfect transceiver RF chains and coarse ADCs/DACs at the users.

Fig. 7 depicts the ergodic secrecy rate versus the quantization bits of low resolution ADCs with different quality of the RF chains. It is observed that increasing the ADCs/DACs quantization precision has a positive effect on the ergodic secrecy rate which can be explained by the fact that the secrecy rate is a monotonically increasing function of ADCs' quantization accuracy. Moreover, it can be noticed that the secrecy rate gradually converges to a fixed limit which is determined by the RF quality. Besides, when $b \geq 5$, the ergodic secrecy rate is extremely close to the finite limit values which is consistent with the conclusion in [26]. This observation indicates that equipping with 5-bit ADCs/DACs leads to an insignificant capacity loss and this is effective enough for practical cell-free massive MIMO system.

Fig. 8 shows the compensation between ADCs/DACs quantization bits b and RF quality factors k where $b_U = b_A = b$ and $k_U = k_A = k$. The curves are obtained by using the proposed compensation algorithm against different achievable secrecy rate. In order to facilitate the comparison, each curve is calculated with initialization setting as $b = 1$ and $k = 1$. As it can be seen, with the increase of the values of b, the proposed compensation algorithm has been operated to

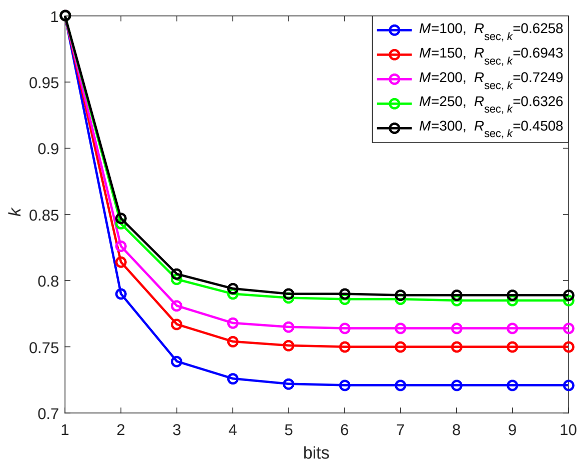

Fig. 8. Illustration of the compensation between ADCs resolution b and RF quality factors k.

determine the corresponding value of k. Each curve in Fig. 8 can achieve the same ergodic secrecy rate, that is, improving the precision of ADCs/DACs can tolerate worse RF chain quality, and vice versa. Hence, these results are extremely valuable and constructive for optimizing the hardware costs and energy efficient in practical system design.

VI. Conclusion

This paper investigated the secure transmission in a cell-free massive MIMO system with RF impairments and low resolution ADCs/DACs in the presence of an active eavesdropper. Using the AQNM and the GRFIM, closed-form expressions of linear MMSE channel estimation and achievable ergodic secrecy rate have been derived with respect to key system parameters, including pilot power, the number of legitimate users and the total antennas, ADCs/DACs quality factors and transceiver RF impairment factors. It is noted that there is nonzero floor on the channel estimation error caused by the low-quality transceivers. Moreover, based on the achievable ergodic secrecy rate expression, the compensation algorithm between RF impairments and ADCs/DACs resolution has been presented in detail which is feasible for flexibly equipping coarse ADCs/DACs and economical RF components in practical system design.

Acknowledgment

This work was supported by the National Natural Science Foundation of China under Grant 61901502 and Grant U19B214.

Appendix

A. Proof of Theorem 1

Based on (8), the post-processing signal $\tilde{\mathbf{y}}_{pm,k'}$ can be rewritten as

$$\begin{aligned}&\tilde{\mathbf{y}}_{pm,k'} = \alpha_A \sum_{k_1\in P_k} \sqrt{\tau p_p k_A k_U}\mathbf{g}_{mk_1} + \\ &\alpha_A\sqrt{k_A}\sum_{k_1=1}^{K}\mathbf{g}_{mk_1}\eta_{k_1 t,k'} + \alpha_A\sqrt{\tau p_E k_A}\mathbf{g}_{mE}\boldsymbol{\varphi}_k^H\boldsymbol{\varphi}_{k'} \\ &+\alpha_A\boldsymbol{\eta}_{mr,k'} + \alpha_A\mathbf{w}_{pm,k'} + \tilde{\mathbf{w}}_{pm,k'}.\end{aligned} \tag{56}$$

It remarks that the different terms are mutually independent of each other and are all Gaussian RVs with zero mean. Based on the linear MMSE algorithm, we can obtain that

$$\hat{\mathbf{g}}_{mk'} = \frac{\mathbb{E}\left\{\tilde{\mathbf{y}}_{pm,k'}^H\mathbf{g}_{mk'}\right\}}{\mathbb{E}\left\{\tilde{\mathbf{y}}_{pm,k'}^H\tilde{\mathbf{y}}_{pm,k'}\right\}}\tilde{\mathbf{y}}_{pm,k'}, \tag{57}$$

First, we focus on the term $\mathbb{E}\left\{\tilde{\mathbf{y}}_{pm,k'}^H\mathbf{g}_{mk'}\right\}$ as

$$\mathbb{E}\left\{\tilde{\mathbf{y}}_{pm,k'}^H\mathbf{g}_{mk'}\right\} = N\alpha_A\sqrt{\tau p_p k_A k_U}\beta_{mk'}. \tag{58}$$

We make a definition that as

$$\begin{aligned}\mathbf{y}_{pm,k'} =& \sum_{k_1\in P_k}\sqrt{\tau p_p k_A k_U}\mathbf{g}_{mk_1} + \sqrt{k_A}\sum_{k_1=1}^{K}\mathbf{g}_{mk_1}\eta_{k_1 t,k'} \\ &+\sqrt{\tau p_E k_A}\mathbf{g}_{mE}\varphi_k^H\varphi_{k'} + \eta_{mr,k'} + \mathbf{w}_{pm,k'}.\end{aligned} \tag{59}$$

As such, we can recast (56) as

$$\tilde{\mathbf{y}}_{pm,k'} = \alpha_A\mathbf{y}_{pm,k'} + \tilde{\mathbf{w}}_{pm,k'}. \tag{60}$$

The covariance of the quantization noise can be given by

$$\mathbb{E}\left\{\mathbf{w}_{pm,k'}^H\mathbf{w}_{pm,k'}\right\} = \alpha_A(1-\alpha_A)\,\mathbb{E}\left\{\mathbf{y}_{pm,k'}^H\mathbf{y}_{pm,k'}\right\}. \tag{61}$$

Hence, we can have that

$$\begin{aligned}\mathbb{E}\left\{\tilde{\mathbf{y}}_{pm,k'}^H\tilde{\mathbf{y}}_{pm,k'}\right\} &= \alpha_A^2\mathbb{E}\left\{\mathbf{y}_{pm,k'}^H\mathbf{y}_{pm,k'}\right\} \\ &+\alpha_A(1-\alpha_A)\,\mathbb{E}\left\{\mathbf{y}_{pm,k'}^H\mathbf{y}_{pm,k'}\right\} \\ &=\alpha_A\mathbb{E}\left\{\mathbf{y}_{pm,k'}^H\mathbf{y}_{pm,k'}\right\}.\end{aligned} \tag{62}$$

According to the definition and statistic properties of different terms in (59), we can derive that

$$\begin{aligned}&\mathbb{E}\left\{\mathbf{y}_{pm,k'}^H\mathbf{y}_{pm,k'}\right\} = \tau p_p k_A k_U\sum_{k_1\in P_k}\mathbb{E}\left\{\|\mathbf{g}_{mk_1}\|^2\right\} + \\ &k_A\sum_{k_1=1}^{K}\mathbb{E}\left\{\|\mathbf{g}_{mk_1}\eta_{k_1 t,k'}\|^2\right\} + \tau p_E k_A\left|\boldsymbol{\varphi}_k^H\boldsymbol{\varphi}_{k'}\right|^2\mathbb{E}\left\{\|\mathbf{g}_{mE}\|^2\right\} \\ &+\mathbb{E}\left\{\|\eta_{mr,k'}\|^2\right\} + \mathbb{E}\left\{\|\mathbf{w}_{pm,k'}\|^2\right\} \\ &= N\rho_p\sum_{k_1=1}^{K}\beta_{mk_1}\left(\tau k_A k_U\left|\boldsymbol{\varphi}_{k'}^H\boldsymbol{\varphi}_{k_1}\right|^2 + 1 - k_A k_U\right) \\ &+\left(\tau k_A\left|\boldsymbol{\varphi}_{k'}^H\boldsymbol{\varphi}_k\right|^2 + 1 - k_A\right)\rho_E\beta_{mE} + \delta^2\end{aligned} \tag{63}$$

Plugging the expressions of (58) and (62) into (57), we can get the expression of $c_{mk'}$ as (11).

Then, the expectation of the norm-square of the channel estimation can be obtained as

$$\begin{aligned}\mathbb{E}\left\{\hat{\mathbf{g}}_{mk'}^H\hat{\mathbf{g}}_{mk'}\right\} &= c_{mk'}^2\mathbb{E}\left\{\tilde{\mathbf{y}}_{pm,k'}^H\tilde{\mathbf{y}}_{pm,k'}\right\}\\ &= N\alpha_A\sqrt{k_Ak_U\tau p_p}c_{mk'}\beta_{mk'}\\ &= N\lambda_{mk'}.\end{aligned} \tag{64}$$

Besides, the estimation and estimation error are uncorrelated, i.e. $\mathbb{E}\left\{\tilde{\mathbf{g}}_{mk'}^H\hat{\mathbf{g}}_{mk'}\right\}=0$. Furthermore, we can calculate that

$$\begin{aligned}\mathbb{E}\left\{\tilde{\mathbf{g}}_{mk'}^H\tilde{\mathbf{g}}_{mk'}\right\} &= \mathbb{E}\left\{\mathbf{g}_{mk'}^H\mathbf{g}_{mk'}\right\}-\mathbb{E}\left\{\hat{\mathbf{g}}_{mk'}^H\hat{\mathbf{g}}_{mk'}\right\}\\ &= N\left(\beta_{mk'}-\lambda_{mk'}\right).\end{aligned} \tag{65}$$

Thus, the proof is completed.

B. Proof of Theorem 2

Firstly, based on the uncorrelated characters of $\hat{\mathbf{g}}_{mk}$ and $\tilde{\mathbf{g}}_{mk}$ along with the used GRFIM and AQNM, desired results can be obtained as follows:

$$\begin{aligned}DS_k &= \mathbb{E}\left\{\alpha_U\sqrt{\rho_dk_Uk_A}\sum_{m=1}^{M}\gamma_{mk}^{1/2}\hat{\mathbf{g}}_{mk}^H\left(\hat{\mathbf{g}}_{mk}+\tilde{\mathbf{g}}_{mk}\right)\right\}\\ &= N\alpha_U\sqrt{\rho_dk_Uk_A}\sum_{m=1}^{M}\gamma_{mk}^{1/2}\lambda_{mk},\end{aligned} \tag{66}$$

$$\mathbb{E}\left\{\left|BU_k\right|^2\right\}=\alpha_U^2\rho_dk_Uk_A\Omega_{kk}-\left|DS_k\right|^2, \tag{67}$$

$$\mathbb{E}\left\{\left|UI_{kk'}\right|^2\right\}=\alpha_U^2\rho_dk_Uk_A\Omega_{kk'}, \tag{68}$$

$$\mathbb{E}\left\{\left|HI_t^{AP}\right|^2\right\}=\alpha_U^2\rho_dk_U\left(1-k_A\right)\sum_{k'=1}^{K}\Psi_{kk'}, \tag{69}$$

$$\begin{aligned}\mathbb{E}\left\{\left|HI_r^{UE}\right|^2\right\} &= \alpha_U^2\rho_d\left(1-k_U\right)\cdot\\ &\left(k_A\sum_{k'=1}^{K}\Omega_{kk'}+\left(1-k_A\right)\sum_{k'=1}^{K}\Psi_{kk'}\right),\end{aligned} \tag{70}$$

$$\mathbb{E}\left\{\left|AN_k\right|^2\right\}=\alpha_U^2\delta^2, \tag{71}$$

$$\begin{aligned}&\mathbb{E}\left\{\left|FN_k\right|^2\right\}=\alpha_U\left(1-\alpha_U\right)\cdot\\ &\left(k_A\rho_d\sum_{m=1}^{M}\Omega_{kk'}+\left(1-k_A\right)\rho_d\sum_{m=1}^{M}\Psi_{kk'}+\delta^2\right).\end{aligned} \tag{72}$$

Then, the term $\Omega_{kk'}$ can be rewritten as

$$\begin{aligned}\Omega_{kk'} &= \mathbb{E}\left\{\left|\sum_{m=1}^{M}\sqrt{\gamma_{mk'}}\hat{\mathbf{g}}_{mk'}^H\mathbf{g}_{mk}\right|^2\right\}\\ &= \mathbb{E}\left\{\left|\sum_{m=1}^{M}c_{mk'}\sqrt{\gamma_{mk'}}\tilde{\mathbf{y}}_{pm,k'}^H\mathbf{g}_{mk}\right|^2\right\}\\ &= \zeta_1+\zeta_2+\zeta_3+\zeta_4+\zeta_5+\zeta_6,\end{aligned} \tag{73}$$

where

$$\begin{aligned}&\zeta_1=\\ &\mathbb{E}\left\{\left|\sum_{m=1}^{M}\alpha_Ac_{mk'}\sqrt{\gamma_{mk'}\tau p_pk_Uk_A}\sum_{k_1=1}^{K}\mathbf{g}_{mk_1}^H\mathbf{g}_{mk}\boldsymbol{\varphi}_{k_1}^H\boldsymbol{\varphi}_{k'}\right|^2\right\},\end{aligned} \tag{74}$$

$$\zeta_2=\mathbb{E}\left\{\left|\sum_{m=1}^{M}\alpha_Ac_{mk'}\sqrt{\gamma_{mk'}k_A}\sum_{k_1=1}^{K}\eta_{k_1t,k'}\mathbf{g}_{mk_1}^H\mathbf{g}_{mk}\right|^2\right\}, \tag{75}$$

$$\zeta_3=\mathbb{E}\left\{\left|\sum_{m=1}^{M}\alpha_Ac_{mk'}\sqrt{\gamma_{mk'}\tau p_Ek_A}\mathbf{g}_{mE}^H\mathbf{g}_{mk}\boldsymbol{\varphi}_k^H\boldsymbol{\varphi}_{k'}\right|^2\right\}, \tag{76}$$

$$\zeta_4=\mathbb{E}\left\{\left|\sum_{m=1}^{M}\sqrt{\gamma_{mk'}}\alpha_Ac_{mk'}\boldsymbol{\eta}_{mr,k'}^H\mathbf{g}_{mk}\right|^2\right\}, \tag{77}$$

$$\zeta_5=\mathbb{E}\left\{\left|\sum_{m=1}^{M}\sqrt{\gamma_{mk'}}\alpha_Ac_{mk'}\mathbf{w}_{pm,k'}^H\mathbf{g}_{mk}\right|^2\right\}, \tag{78}$$

$$\zeta_6=\mathbb{E}\left\{\left|\sum_{m=1}^{M}\sqrt{\gamma_{mk'}}c_{mk'}\tilde{\mathbf{w}}_{pm,k'}^H\mathbf{g}_{mk}\right|^2\right\}. \tag{79}$$

Then, some algebraic manipulations should be presented to compute the above terms respectively as

$$\begin{aligned}&\zeta_1=\alpha_A^2\tau p_pk_Uk_A\left(\mathbb{E}\left\{\left|\sum_{m=1}^{M}c_{mk'}\sqrt{\gamma_{mk'}}\mathbf{g}_{mk}^H\mathbf{g}_{mk}\boldsymbol{\varphi}_k^H\boldsymbol{\varphi}_{k'}\right|^2\right\}\right.\\ &\left.+\mathbb{E}\left\{\left|\sum_{m=1}^{M}c_{mk'}\sqrt{\gamma_{mk'}}\sum_{k_1\neq k}^{K}\mathbf{g}_{mk_1}^H\mathbf{g}_{mk}\boldsymbol{\varphi}_{k_1}^H\boldsymbol{\varphi}_{k'}\right|^2\right\}\right)\\ &=\alpha_A^2\tau p_pk_Uk_A\left(N^2\left(\sum_{m=1}^{M}c_{mk'}\sqrt{\gamma_{mk'}}\beta_{mk}\right)^2\right.\\ &\left.+N\sum_{m=1}^{M}c_{mk'}^2\gamma_{mk'}\beta_{mk}^2\right)\cdot\left|\boldsymbol{\varphi}_k^H\boldsymbol{\varphi}_{k'}\right|^2+\\ &N\alpha_A^2\tau p_pk_Uk_AN\sum_{m=1}^{M}\sum_{k_1\neq k}^{K}c_{mk'}^2\gamma_{mk'}\beta_{mk_1}\beta_{mk}\cdot\left|\boldsymbol{\varphi}_{k_1}^H\boldsymbol{\varphi}_{k'}\right|^2\\ &=\alpha_A^2\tau p_pk_Uk_A\cdot\left(N^2\left(\sum_{m=1}^{M}c_{mk'}\sqrt{\gamma_{mk'}}\beta_{mk}\right)^2\cdot\left|\boldsymbol{\varphi}_k^H\boldsymbol{\varphi}_{k'}\right|^2\right.\\ &\left.+N\sum_{m=1}^{M}\sum_{k_1=1}^{K}c_{mk'}^2\gamma_{mk'}\beta_{mk_1}\beta_{mk}\cdot\left|\boldsymbol{\varphi}_{k_1}^H\boldsymbol{\varphi}_{k'}\right|^2\right),\end{aligned} \tag{80}$$

$$\begin{aligned}\zeta_2 &= k_A\alpha_A^2\mathbb{E}\left\{\left|\sum_{m=1}^{M} c_{mk'}\sqrt{\gamma_{mk'}}\|\mathbf{g}_{mk}\|^2\eta_{k_1t,k}\right|^2\right\}+\\ &k_A\alpha_A^2\mathbb{E}\left\{\left|\sum_{m=1}^{M} c_{mk'}\sqrt{\gamma_{mk'}}\sum_{k_1\neq k}^{K}\eta_{k_1t,k'}\mathbf{g}_{mk_1}^H\mathbf{g}_{mk}\right|^2\right\}\\ &= k_A\left(1-k_U\right)\alpha_A^2\left(N^2\left(\sum_{m=1}^{M} c_{mk'}^2\gamma_{mk'}\beta_{mk}\right)^2\right.\\ &\left.+N\sum_{m=1}^{M} c_{mk'}\sqrt{\gamma_{mk'}}\sum_{k_1=1}^{K} c_{mk'}^2\gamma_{mk'}\beta_{mk_1}\beta_{mk}\right),\end{aligned} \tag{81}$$

$$\zeta_3 = \alpha_A^2\tau p_E k_A\sum_{m=1}^{M} c_{mk'}^2\gamma_{mk'}\beta_{mE}\beta_{mk}\cdot\left|\boldsymbol{\varphi}_k^H\boldsymbol{\varphi}_{k'}\right|^2, \tag{82}$$

$$\begin{aligned}&\zeta_4 = N\alpha_A^2\left(1-k_A\right)\cdot\\ &\sum_{m=1}^{M} c_{mk'}^2\gamma_{mk'}\left(p_p\beta_{mk}^2+p_p\sum_{k_1=1}^{K}\beta_{mk_1}\beta_{mk}+p_E\beta_{mE}\beta_{mk}\right),\end{aligned} \tag{83}$$

$$\zeta_5 = \alpha_A^2\delta^2\sum_{m=1}^{M} c_{mk'}^2\gamma_{mk'}\beta_{mk}, \tag{84}$$

$$\begin{aligned}\zeta_6 &= N\alpha_A\left(1-\alpha_A\right)\sum_{m=1}^{M}\frac{c_{mk'}^2\gamma_{mk'}\beta_{mk}\beta_{mk'}\sqrt{\tau\rho_p k_A k_U}}{c_{mk'}}\\ &= N\left(1-\alpha_A\right)\sum_{m=1}^{M}\gamma_{mk'}\lambda_{mk'}\beta_{mk}.\end{aligned} \tag{85}$$

Now, plugging these results into (73), we can get the analytical result in (31) with some linear algebraic manipulations. Besides, utilizing the similar methodology, the expression of (32) can be achieved by some algebraic operations. Finally, by substituting the expressions of $\Omega_{kk'}$ and $\Psi_{kk'}$ into (36), (37), (38) and (40), the desired closed-form results of (33) as well as the ergodic rate of the kth user can be obtained. This finishes the proof.

C. Proof of Theorem 3

In order to obtain the closed-form expression of the ergodic capacity of the Eve, it is noted that it is crucial to calculate the terms of $\Omega_{Ek'}$ and $\Psi_{Ek'}$. Now, we can rewrite $\Omega_{Ek'}$ as

$$\begin{aligned}\Omega_{Ek'} &= \mathbb{E}\left\{\left|\sum_{m=1}^{M} c_{mk'}\sqrt{\gamma_{mk'}}\tilde{\mathbf{y}}_{pm,k'}^H\mathbf{g}_{mE}\right|^2\right\}\\ &= \varepsilon_1+\varepsilon_2+\varepsilon_3+\varepsilon_4+\varepsilon_5+\varepsilon_6,\end{aligned} \tag{86}$$

where

$$\begin{aligned}&\varepsilon_1 =\\ &\mathbb{E}\left\{\left|\sum_{m=1}^{M}\alpha_A c_{mk'}\sqrt{\gamma_{mk'}\tau p_p k_U k_A}\sum_{k_1=1}^{K}\mathbf{g}_{mk_1}^H\mathbf{g}_{mE}\boldsymbol{\varphi}_{k_1}^H\boldsymbol{\varphi}_{k'}\right|^2\right\},\end{aligned} \tag{87}$$

$$\begin{aligned}&\varepsilon_2 =\\ &\mathbb{E}\left\{\left|\sum_{m=1}^{M}\alpha_A c_{mk'}\sqrt{\gamma_{mk'}k_A}\sum_{k_1=1}^{K}\eta_{k_1t,k'}\mathbf{g}_{mk_1}^H\mathbf{g}_{mE}\right|^2\right\},\end{aligned} \tag{88}$$

$$\begin{aligned}&\varepsilon_3 =\\ &\mathbb{E}\left\{\left|\sum_{m=1}^{M}\alpha_A c_{mk'}\sqrt{\gamma_{mk'}\tau p_E k_A}\mathbf{g}_{mE}^H\mathbf{g}_{mE}\boldsymbol{\varphi}_k^H\boldsymbol{\varphi}_{k'}\right|^2\right\},\end{aligned} \tag{89}$$

$$\varepsilon_4 = \mathbb{E}\left\{\left|\sum_{m=1}^{M}\alpha_A c_{mk'}\eta_{mr,k'}^H\mathbf{g}_{mE}\right|^2\right\}, \tag{90}$$

$$\varepsilon_5 = \mathbb{E}\left\{\left|\sum_{m=1}^{M}\alpha_A c_{mk'}\mathbf{w}_{pm,k'}^H\mathbf{g}_{mE}\right|^2\right\}, \tag{91}$$

$$\varepsilon_6 = \mathbb{E}\left\{\left|\sum_{m=1}^{M} c_{mk'}\tilde{\mathbf{w}}_{pm,k'}^H\mathbf{g}_{mE}\right|^2\right\}. \tag{92}$$

Due to the mutual independence between $\mathbf{g}_{mE}$ and $\mathbf{g}_{mi}$ $(1\leq i\leq K)$, the terms in (86) can be computed by

$$\begin{aligned}&\varepsilon_1 =\\ &N\alpha_A^2\tau p_p k_U k_A\sum_{m=1}^{M}\sum_{k_1=1}^{K} c_{mk'}^2\gamma_{mk'}\beta_{mk_1}\cdot\left|\boldsymbol{\varphi}_{k_1}^H\boldsymbol{\varphi}_{k'}\right|^2,\end{aligned} \tag{93}$$

$$\begin{aligned}\varepsilon_2 =&N\alpha_A^2 p_p k_A\left(1-k_U\right)\cdot\\ &\sum_{m=1}^{M}\sqrt{k_A}\sum_{k_1=1}^{K} c_{mk'}^2\gamma_{mk'}\beta_{mk_1}\beta_{mE},\end{aligned} \tag{94}$$

$$\begin{aligned}\varepsilon_3 =&N^2\alpha_A^2 k_A\tau p_E\left|\boldsymbol{\varphi}_{k'}^H\boldsymbol{\varphi}_k\right|^2\left(\sum_{m=1}^{M} c_{mk'}\sqrt{\gamma_{mk'}}\beta_{mE}\right)^2\\ &+N\alpha_A^2 k_A\tau p_E\left|\boldsymbol{\varphi}_{k'}^H\boldsymbol{\varphi}_k\right|^2\sum_{m=1}^{M} c_{mk'}^2\gamma_{mk'}\beta_{mE}^2,\end{aligned} \tag{95}$$

$$\begin{aligned}\varepsilon_4 &= \mathbb{E}\left\{\left|\sum_{m=1}^{M}\alpha_A c_{mk'}\eta_{mr,k'}^H\mathbf{g}_{mE}\right|^2\right\}\\ &= N\alpha_A^2\left(1-k_A\right)\cdot\\ &\sum_{m=1}^{M} c_{mk'}^2\left(\sum_{k_1=1}^{K} p_p\beta_{mk_1}\beta_{mE}+2p_E\beta_{mE}^2\right),\end{aligned} \tag{96}$$

$$\varepsilon_5 = N\alpha_A^2\sum_{m=1}^{M} c_{mk'}^2\delta^2\beta_{mE}, \tag{97}$$

$$\begin{aligned}\varepsilon_6 &= N\alpha_A\left(1-\alpha_A\right)\cdot\\ &\sum_{m=1}^{M}\frac{c_{mk'}^2\gamma_{mk'}\beta_{mE}\beta_{mk'}\sqrt{\tau\rho_p k_A k_U}}{c_{mk'}}\\ &= N\left(1-\alpha_A\right)\sum_{m=1}^{M}\gamma_{mk'}\lambda_{mk'}\beta_{mE}.\end{aligned} \tag{98}$$

Then, substituting the above six terms into (86), we can get the result as (45). With the same algebraic manipulations, the expressions of (46) and (47) as well as the ergodic capacity of the Eve can be derived, which can complete the proof.

References

[1] T. L. Marzetta, "Massive MIMO: an introduction," *Bell Labs Techn. J.*, vol. 20, no. 2015, pp. 11-20, Mar. 2015.

[2] E. G. Larsson, O. Edfors, F. Tufvesson, and T. L. Marzetta, "Massive MIMO for next generation wireless systems," *IEEE Commun. Mag.*, vol. 52, no. 2, pp. 186-195, Feb. 2014.

[3] J. Zhang, C. Wen, S. Jin, X. Gao, and K. Wong, "On Capacity of Large-Scale MIMO Multiple Access Channels with Distributed Sets of Correlated Antennas," *IEEE J. Sel. Areas Commun.*, vol. 31, no. 2, pp. 133-148, Feb. 2013.

[4] A. Yang, Y. Jing, C. Xing, Z. Fei, and J. Kuang, "Performance Analysis and Location Optimization for Massive MIMO Systems With Circularly Distributed Antennas," *IEEE Trans. Wireless Commun.*, vol. 14, no. 10, pp. 5659-5671, Oct. 2015.

[5] H. Q. Ngo, A. Ashikhmin, H. Yang, E. G. Larsson, and T. L. Marzetta, "cell-free Massive MIMO Versus Small Cells," *IEEE Trans. Wireless Commun.*, vol. 16, no. 3, pp. 1834-1850, Mar. 2017.

[6] H. Q. Ngo, L. Tran, T. Q. Duong, M. Matthaiou, and E. G. Larsson, "On the Total Energy Efficiency of cell-free Massive MIMO," *IEEE Trans. Green Commun. Netw.*, vol. 2, no. 1, pp. 25-39, Mar. 2018.

[7] A. Papazafeiropoulos, P. Kourtessis, M. D. Renzo, S. Chatzinotas, and J. M. Senior, "Performance Analysis of Cell-Free Massive MIMO Systems: A Stochastic Geometry Approach," *IEEE Trans. Veh. Technol.*, vol. 69, no. 4, pp. 3523-3537, Apr. 2020.

[8] H. V. Nguyen, V. Nguyen, O. A. Dobre, et al., "On the Spectral and Energy Efficiencies of Full-Duplex Cell-Free Massive MIMO," *IEEE J. Sel. Areas Commun.*, vol. 38, no. 8, pp. 1698-1718, Aug. 2020.

[9] A. K. Papazafeiropoulos, P. Kourtessis, S. Chatzinotas, and J. M. Senior, "Multipair Two-Way DF Relaying With Cell-Free Massive MIMO," *IEEE Open J. Commun. Society*, vol. 2, pp. 423-438, Mar. 2021.

[10] A. Papazafeiropoulos, H. Q. Ngo, P. Kourtessis, S. Chatzinotas, and J. M. Senior, "Towards Optimal Energy Efficiency in Cell-Free Massive MIMO Systems," *IEEE Trans. Green Commun. Netw.*, [Online] doi:10.1109/TGCN.2021.3059206.

[11] N. Yang, L. Wang, G. Geraci, M. Elkashlan, J. Yuan and M. Di Renzo, "Safeguarding 5G wireless communication networks using physical layer security," *IEEE Commun. Mag.*, vol. 53, no. 4, pp. 20-27, Apr. 2015.

[12] Y. P. Hong, P. Lan, and C. J. Kuo, "Enhancing Physical-Layer Secrecy in Multiantenna Wireless Systems: An Overview of Signal Processing Approaches," *IEEE Signal Process. Mag.*, vol. 30, no. 5, pp. 29-40, Sept. 2013.

[13] D. Kapetanovic, G. Zheng, and F. Rusek, "Physical layer security for massive MIMO: An overview on passive eavesdropping and active attacks," *IEEE Commun. Mag.*, vol. 53, no. 6, pp. 21-27, Jun. 2015.

[14] Y. Wu, R. Schober, D. W. K. Ng, C. Xiao, and G. Caire, "Secure Massive MIMO Transmission With an Active Eavesdropper," *IEEE Trans. Inf. Theory*, vol. 62, no. 7, pp. 3880-3900, Jul. 2016.

[15] J. Zhu, R. Schober, and V. K. Bhargava, "Secure Transmission in Multicell Massive MIMO Systems," *IEEE Trans. Wireless Commun.*, vol. 13, no. 9, pp. 4766-4781, Sept. 2014.

[16] Y. Wu, R. Schober, D. W. K. Ng, C. Xiao, and G. Caire, "Secure Massive MIMO Transmission With an Active Eavesdropper," *IEEE Trans. Inf. Theory*, vol. 62, no. 7, pp. 3880-3900, Jul. 2016.

[17] X. Zhang, D. Guo, K. Guo, and H. Niu, "Secure performance analysis and detection of pilot attack in massive multiple-input multiple-output system," *Int. J. Distrib. Sensor Netw.*, vol. 14, no. 5, May 2018.

[18] X. Zhang, D. Guo, K. An, X. Liang, and W. Ma, "Secure Transmission in Multi-Pair AF Relaying Massive MIMO Networks Against Active Pilot Spoofing Attacks," *IEEE Access*, vol. 7, pp. 3547-3560, Jan. 2019.

[19] K. Guo, Y. Guo, and G. Ascheid, "Security-Constrained Power Allocation in MU-Massive-MIMO With Distributed Antennas," *IEEE Trans. Wireless Commun.*, vol. 15, no. 12, pp. 8139-8153, Dec. 2016.

[20] X. Zhang, D. Guo, K. An, W. Ma, and K. Guo, "Secure transmission and power allocation in multiuser distributed massive MIMO systems," *Wireless Netw.*, vol. 26, pp. 941-954, Feb. 2020.

[21] T. M. Hoang, H. Q. Ngo, T. Q. Duong, H. D. Tuan, and A. Marshall, "cell-free Massive MIMO Networks: Optimal Power Control Against Active Eavesdropping," *IEEE Trans. Commun.*, vol. 66, no. 10, pp. 4724-4737, Oct. 2018.

[22] X. Zhang, D. Guo, K. An, Z. Ding, and B. Zhang, "Secrecy Analysis and Active Pilot Spoofing Attack Detection for Multigroup Multicasting cell-free Massive MIMO Systems," *IEEE Access*, vol. 7, pp. 57332-57340, May 2019.

[23] M. Alageli, A. Ikhlef, F. Alsifiany, M. A. M. Abdullah, G. Chen and J. Chambers, "Optimal Downlink Transmission for cell-free SWIPT Massive MIMO Systems With Active Eavesdropping," *IEEE Trans. Inf. Forensics Secur.*, vol. 15, no. 1, pp. 1983-1998, Jan. 2020.

[24] J. Zhu, D. W. K. Ng, N. Wang, R. Schober, and V. K. Bhargava, "Analysis and Design of Secure Massive MIMO Systems in the Presence of Hardware Impairments," *IEEE Trans. Wireless Commun.*, vol. 16, no. 3, pp. 2001-2016, Mar. 2017.

[25] J. Zhu, Y. Li, N. Wang, and W. Xu, "Wireless Information and Power Transfer in Secure Massive MIMO Downlink With Phase Noise," *IEEE Wireless Commun. Lett.*, vol. 6, no. 3, pp. 298-301, Jun. 2017.

[26] X. Zhang, D. Guo, K. An, and B. Zhang, "Secure Communications Over cell-free Massive MIMO Networks With Hardware Impairments," *IEEE Syst. J.*, vol. 14, no. 2, pp. 1909-1920, Jun. 2020.

[27] Q. Xu, and P. Ren, "Secure Massive MIMO Downlink With Low-Resolution ADCs/DACs in the Presence of Active Eavesdropping," *IEEE Access*, vol. 8, pp. 140981-140997, Aug. 2020.

[28] E. Björnson, J. Hoydis, M. Kountouris, and M. Debbah, "Massive MIMO Systems With Non-Ideal Hardware: Energy Efficiency, Estimation, and Capacity Limits," *IEEE Trans. Inf. Theory*, vol. 60, no. 11, pp. 7112-7139, Nov. 2014.

[29] L. Xu, X. Lu, S. Jin, F. Gao, and Y. Zhu, "On the Uplink Achievable Rate of Massive MIMO System with Low-Resolution ADC and RF Impairments," *IEEE Commun. Lett.*, vol. 23, no. 3, pp. 502-505, Mar. 2019.

[30] Y. Zhang, M. Zhou, Y. Cheng, L. Yang, and H. Zhu, "RF Impairments and Low-Resolution ADCs for Nonideal Uplink cell-free Massive MIMO Systems," *IEEE Syst. J.*, [Online] Doi:10.1109/JSYST.2020.2990709

[31] X. Hu, C. Zhong, X. Chen, W. Xu, H. Lin, and Z. Zhang, "cell-free Massive MIMO Systems With Low Resolution ADCs," *IEEE Trans. Commun.*, vol. 67, no. 10, pp. 6844-6857, Oct. 2019.

[32] J. Zhang, Y. Wei, E. Björnson, Y. Han, and S. Jin, "Performance Analysis and Power Control of cell-free Massive MIMO Systems With Hardware Impairments," *IEEE Access*, vol. 6, pp. 55302-55314, Oct. 2018.

[33] A. K. Fletcher, S. Rangan, V. K. Goyal, and K. Ramchandran, "Robust Predictive Quantization: Analysis and Design Via Convex Optimization," *IEEE J. Sel. Topics Signal Process.*, vol. 1, no. 4, pp. 618-632, Dec. 2007.

[34] O. T. Demir, and E. Björnson, "The Bussgang Decomposition of Nonlinear Systems: Basic Theory and MIMO Extensions [Lecture Notes]," *IEEE Signal Process Mag.*, vol. 38, no. 1, pp. 131-136, Jan. 2021.

[35] Y. Zhang, M. Zhou, X. Qiao, H. Cao and L. Yang, "On the Performance of Cell-Free Massive MIMO With Low-Resolution ADCs," *IEEE Access*, vol. 7, pp. 117968-117977, Sept. 2019.